ISBN: 978-3-95450-234-9 ISSN: 2673-5504 doi:10.18429/JACoW-SRF2023-MOPMB050

THERMAL FEEDBACK IN COAXIAL SRF CAVITIES*

M. W. McMullin†[1], T. Junginger[1], P. Kolb, R. E. Laxdal, Z. Yao, TRIUMF, Vancouver, BC, Canada
[1]also at Department of Physics & Astronomy, University of Victoria, Victoria, BC, Canada

Abstract

The phenomenon of Q-slope in SRF cavities is caused by a combination of thermal feedback and field-dependent surface resistance. There is currently no commonly accepted model of field-dependent surface resistance, and studies of Q-slope generally treat thermal feedback as a correction to whichever surface resistance model is being used. In the present study, we treat thermal feedback as a distinct physical effect whose effect on Q-slope is calculated using a novel finite-element code. We performed direct measurements of liquid helium pool boiling from niobium surfaces to obtain input parameters for the finite-element code. This code was used to analyze data from TRIUMF's coaxial test cavity program, which has provided a rich dataset of Q-curves at temperatures between 1.7 K and 4.4 K at five different frequencies. Preliminary results show that thermal feedback makes only a small contribution to Q-slope at temperatures near 4.2 K, but has stronger effects as the bath temperature is lowered.

THERMAL FEEDBACK (TFB) ABOVE T_λ

During operation, the walls of an SRF cavity are constantly heated by the RF power density

$$q = \frac{1}{2} R_s H^2$$

on the inner surface of the cavity. Because of the finite thermal conductivity of niobium and imperfect cooling by the helium bath, the RF surface of the cavity is always warmer than the helium bath, and the difference in temperature increases with q (see Fig. 1). This heating in turn increases the temperature-dependent part of the surface resistance, further increasing q to create a feedback loop. The feedback loop results either in unbounded heating, quenching the cavity, or in steady-state operation with an increased dynamic heat load.

Because of thermal feedback (TFB), the total power P dissipated in the cavity increases faster than the square of the field strength, quantified by the peak surface magnetic field B_p. Since the energy U stored in the cavity fields is proportional to B_p^2, the quality factor

$$Q_0 = \frac{\omega U}{P} \tag{1}$$

decreases with an increase in B_p. Therefore, TFB impacts measured Q-slope whether or not R_s is itself dependent on the applied field. The thermal conductivity of the cavity walls and efficiency of heat transfer to the helium bath determine the amount of Q-slope that comes from TFB as opposed to intrinsic field dependence of R_s.

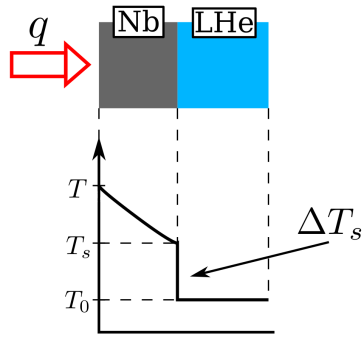

Figure 1: Cross section showing the temperature gradient across the wall of an SRF cavity.

Measurements on a quarter-wave and half-wave resonator (QWR and HWR) in TRIUMF's coaxial test cavity program (detailed in Ref. [1], HWR shown in Fig. 2) show signs that TFB is a non-negligible effect. These measurements are separated into sets of Q_0 vs. B_p curves taken repeatedly in a single cavity mode while cooling the helium bath from about 4.4 K to 2.0-1.7 K. Below $T_\lambda = 2.177$ K, the surface resistance drops abruptly, as shown in Fig. 3, and the size of the drop grows with B_p. This drop is believed to occur because the helium bath enters a superfluid state and cooling is significantly enhanced, mitigating TFB. Measurements of niobium cooling in superfluid helium have previously been conducted and integrated into studies of Q-slope [2–4], but TFB above T_λ has not been extensively studied because of the lack of data on cooling at the niobium-helium interface in the normal fluid regime.

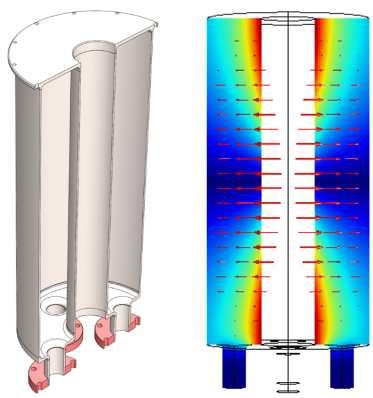

Figure 2: Model (left) and field distribution in the fundamental 389 MHz mode (right) for the HWR in Ref. [1].

* Work supported by the National Research Council Canada
† mmcmullin@triumf.ca

ISBN: 978-3-95450-234-9 ISSN: 2673-5504 doi:10.18429/JACoW-SRF2023-MOPMB050

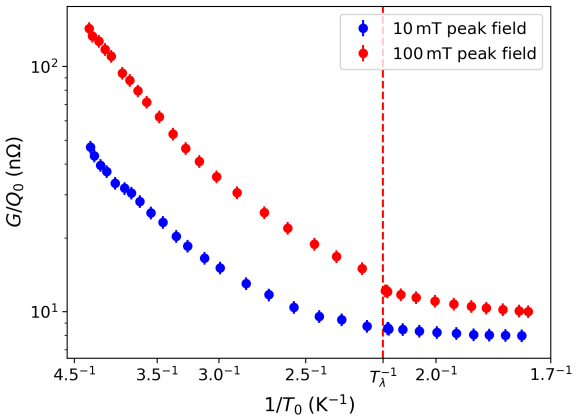

Figure 3: Average surface resistance G/Q_0 vs. inverse bath temperature $1/T_0$ for the 120 °C baked HWR at 389 MHz. Note the jump in surface resistance at T_λ at $B_p = 100$ mT.

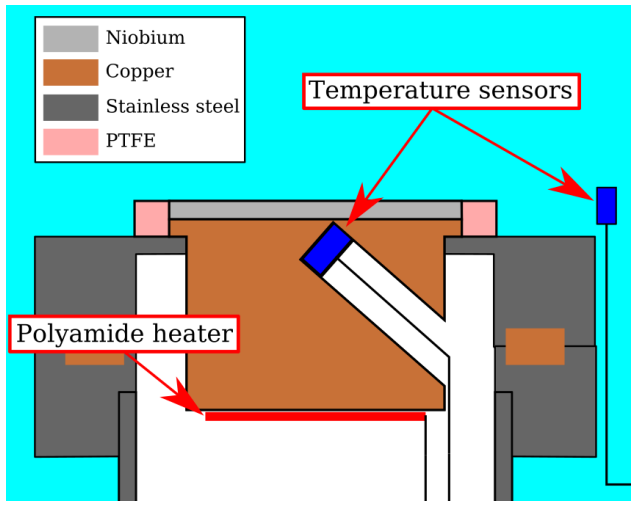

Figure 4: Schematic of the test setup for boiling curve measurements.

The present study was undertaken in order to determine the impact of TFB on Q-slope observed in TRIUMF's coaxial cavity dataset above T_λ. To fill the gap in the literature, novel measurements of boiling from niobium surfaces in liquid helium were carried out. To apply these measurements to the TFB problem, a custom finite-element based fitting tool was developed to fit field-dependent models of R_s to measured Q-curves while taking into account the full heat flow problem in the coaxial cavities.

Nb-LHe BOILING CURVE MEASUREMENT

Background

The heat flux q through a surface cooled by saturated liquid is determined by the temperature difference between the surface and the liquid, ΔT_s. At very low heat fluxes, the surface is cooled by natural convection and q and ΔT_s are roughly proportional to one another. As the heat flux increases, bubbles start to form at nucleation sites, marking the start of the nucleate boiling regime. As more nucleation sites become active, heat transfer grows more efficient (lower ΔT_s for a given q) until the density of active nucleation sites saturates. If the heat flux is made sufficiently high, the bubbles will coalesce into a film. This regime, film boiling, is characterized by very poor heat transfer and is not relevant to the performance of unquenched SRF cavities. If the heat flux is instead decreased after reaching the developed nucleate boiling regime, some nucleation sites will remain active until very low heat fluxes. Heat transfer will be more efficient for decreasing heat flux than for increasing, creating some degree of hysteresis in the relationship between q and ΔT_s.

The relationship between q and ΔT_s described above is called a boiling curve. Boiling curves are qualitatively similar for any pairing of working fluid and surface, but a quantitative description of heat transfer depends on the fluid being used, its temperature, and characteristics of the boiling surface like material, roughness, shape, and orientation. In the case of SRF cavities, the working fluid is saturated liquid helium between 2.177 K and 4.3 K and the surface is flat, high-purity niobium sheet. No measurements of boiling curves for a niobium surface of any kind in liquid helium have been reported in the literature.

Measurements

To produce a suitable sample for the boiling measurement, a sheet of 2.1 mm thick rolled niobium with RRR > 250 was bonded to a 1" thick C10100 copper base plate by explosion welding. A cylinder with a diameter of 34 mm was cut from this bonded block and the surface was turned on a lathe to remove irregularities from the welding process. The sample cylinder was soldered to a 2.75" CF flange with a small portion of the sides of the cylinder exposed on the top of the flange. The exposed portion of the sides was covered with a PTFE ring to prevent contact with helium. A hole was drilled in the copper block for mounting a thermometer, as shown in Fig. 4.

During the measurement, heat is applied by a polyamide heater on the bottom of the copper block. The thick copper backing smooths out temperature variations across the niobium disc and functions as an isotherm for measuring the temperature of the niobium at the Nb-Cu weld. The total heat dissipated by the polyamide heater can be precisely controlled. Most of the heater power passes through the niobium surface into the helium bath, but some portion is lost to the system, primarily through the mounting flange. The system heat losses were quantified by a calibration measurement in which the niobium surface was covered by a thick PTFE block. By covering the surface, all heater power is assumed to be lost to the system. A relationship between the copper block temperature and the system heat losses was established by varying the heater power and recording the steady-state response of the sample temperature sensor.

ISBN: 978-3-95450-234-9 ISSN: 2673-5504 doi:10.18429/JACoW-SRF2023-MOPMB050

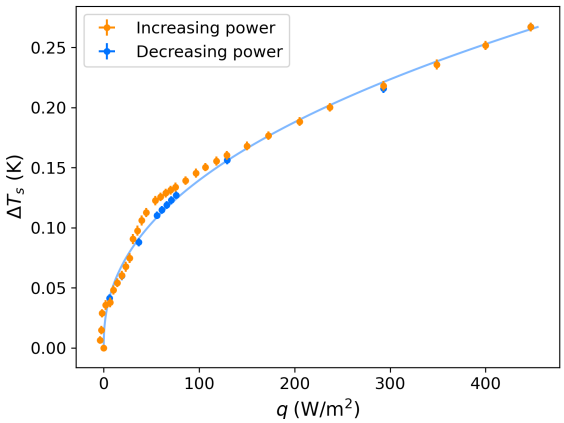

Figure 5: A boiling curve at 4.2 K with the surface normal pointing upwards. This curve displays the most hysteresis of any boiling curves collected in our measurements. The curve fit is from Eq. (2) with parameters listed in in Table 1 for cooldown "Up".

Boiling curves are measured by ramping the heater power up and down in discrete steps, while letting the system settle to a steady state before changing heater power. After subtracting the calibrated system heat losses, the heat flux q through the niobium surface is known at each step. A small correction based on literature data for niobium thermal conductivity [5] is applied to calculate the boiling surface temperature. Together with the readings from the bath temperature sensor, this produces a ΔT_s corresponding to each q in the ramp, yielding a boiling curve. An example of a boiling curve measured in this way is shown in Fig. 5.

Boiling curves were measured at bath temperatures of 4.2 K, 2.5 K, and 2.2 K. The sample housing was rotated to measure boiling curves at these temperatures with the surface normal facing upwards, sideways, and downwards, although no 2.2 K curves were measured with the Nb sample surface facing upwards. Hysteresis was observed in some but not all boiling curves, and the width of hysteresis was small and limited to a narrow range of heat fluxes, as shown in Fig. 5. Within the same cooldown, boiling curves at one temperature were typically collected two or three times and were always found to be repeatable within experimental uncertainties.

For a given heat flux q, the steady-state ΔT_s is larger for lower bath temperature (see Fig. 6), meaning that heat transfer is less efficient at lower temperatures. Figure 7 shows that as the surface is rotated to the downwards facing position, heat transfer becomes more efficient. This commonly observed feature in boiling curve studies is usually attributed to the increased disturbance of the superheated liquid layer by bubbles sliding along the surface [6].

To use measured boiling curves in calculations of thermal feedback, it is useful to make a continuous interpolation of the data. This is done by fitting the function

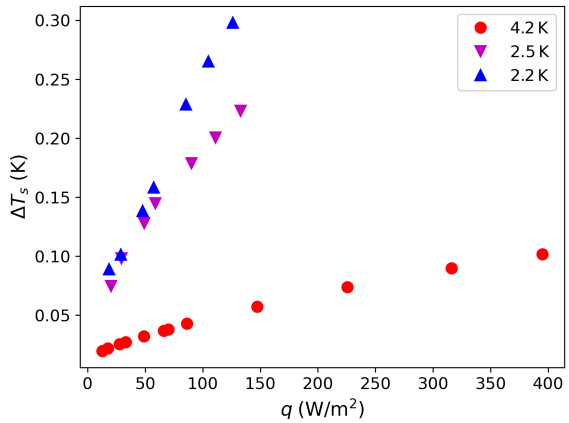

Figure 6: Decreasing portions of curves taken at 4.2 K, 2.5 K, and 2.2 K from the dataset "Side" in Table 1.

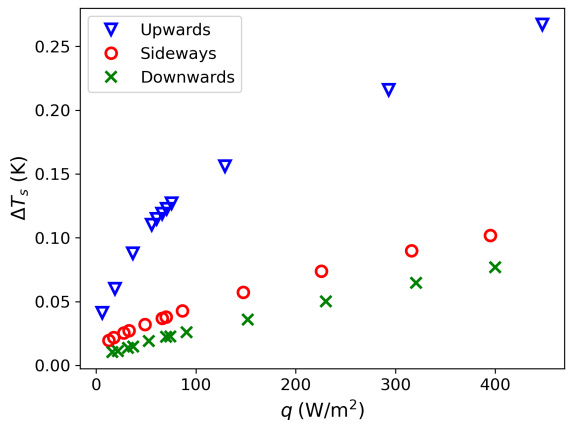

Figure 7: Decreasing portions of curves taken at 4.2 K for three orientations of the surface normal.

$$q = a(\Delta T_s)^n \tag{2}$$

to the decreasing portion of each boiling curve. The decreasing portion is chosen over the increasing because it better represents a condition of developed boiling relevant to SRF cavity performance, but the difference between the two is generally small. Table 1 shows the fit parameters for representative boiling curves from each orientation.

FINITE-ELEMENT METHODS AND TFB

Assuming that the thermal conductivity is uniform, the temperature distribution in cavity walls must satisfy the steady-state heat equation

$$\nabla^2 T = 0. \tag{3}$$

The boundary conditions are defined by a heat flux

$$q = \frac{1}{2} R_s H^2 \tag{4}$$

ISBN: 978-3-95450-234-9 ISSN: 2673-5504 doi:10.18429/JACoW-SRF2023-MOPMB050

Table 1: Boiling Curve Fit Parameters

Cooldown name	T_0 (K)	$a\ \left(\frac{\mathrm{W}}{\mathrm{m}^2\cdot\mathrm{K}^n}\right)$	n
Up	4.26	9900 ± 100	2.33 ± 0.01
	2.54	400 ± 10	1.33 ± 0.03
Side	4.24	21300 ± 400	1.73 ± 0.01
	2.53	2100 ± 100	1.82 ± 0.03
	2.24	570 ± 20	1.26 ± 0.02
Down	4.25	13400 ± 200	1.36 ± 0.01
	2.53	2270 ± 90	1.41 ± 0.02
	2.25	1690 ± 60	1.5 ± 0.02

entering the walls on the the RF side and a heat flux

$$q = h(T_s, T_0)\Delta T_s \tag{5}$$

leaving the walls on the helium side. Here

$$h = \frac{q}{\Delta T_s}$$

can be calculated for each surface orientation from measured boiling curve data. The surface resistance R_s can be any function of the RF surface temperature and field amplitude. The thermal conductivity is calculated using the parameterization of [5] evaluated at the bath temperature T_0.

If the field distribution on the cavity is reasonably uniform, like in elliptical cavities, then Eq. (3) can be reduced to a 1D problem as in [3, 7]. For coaxial cavities, the highly non-uniform field distribution requires that Eq. (3) be solved in 2D with the boundary conditions, defined in Eqs. (4) and (5), allowed to vary on the cavity surfaces.

To solve Eq. (3) a finite-element method based on the Ritz-Galerkin approach is used [8]. The cavity domain is partitioned into a mesh of triangular finite elements. The temperatures at the vertices of the mesh are stored in a column vector **T** that can be found by solving a matrix equation of the form

$$(\mathbf{M} - \mathbf{B}) \cdot \mathbf{T} = \mathbf{p}_{\mathrm{RF}} + \mathbf{b}. \tag{6}$$

Here **M** is a matrix that depends only on the geometry of the mesh, $\mathbf{p}_{\mathrm{RF}}$ is a column vector calculated from the distribution of RF power from Eq. (4) on the cavity surface, and **B** and **b** are a matrix and column vector, respectively, representing the helium side boundary condition of Eq. (5).

Solving Eq. (6) yields the temperature distribution **T** at thermal equilibrium for given **B**, **b**, and $\mathbf{p}_{\mathrm{RF}}$ (see Fig. 8). The boundary conditions, defined by the distribution of R_s and h on the cavity surfaces, are then updated and **B**, **b**, and $\mathbf{p}_{\mathrm{RF}}$ are recalculated. The solution process is repeated until the total power P dissipated inside the cavity converges.

When the solution has converged, the quality factor Q_0 is calculated using Eq. (1). Two functions, one for the HWR and one for the QWR, were written in Julia to calculate Q_0 for a given surface resistance function R_s and a tuple of (ω, B_p, T_0). Solving the TFB problem and calculating Q_0 is fast enough that these functions can be readily used in routines for fitting parameters of a surface resistance model to sets of (ω, B_p, T_0, Q_0) tuples, like the coaxial cavity cooldown datasets.

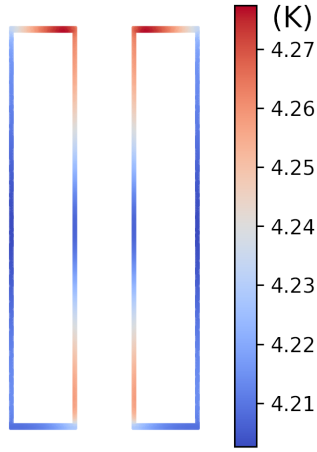

Figure 8: Equilibrium temperature distribution 389 MHz mode of the HWR and typical R_s values. Because boiling is more efficient for surfaces facing downwards than upwards (Fig. 7), the top plate is warmer than the bottom.

The finite-element fitting tool described above allows us to check whether the jump in R_s at T_λ shown in Fig. 3 is explained by TFB. This jump stems from a change in the slope of the Q vs. B_p curve when the bath temperature drops below T_λ. To parametrize Q-slope, we will use the surface resistance function

$$R_s(T,B) = \left(1 + \gamma_0 \left[\frac{B}{B_0}\right]^2\right) R_0 + \left(1 + \gamma \left[\frac{B}{B_0}\right]^2\right) R_{\mathrm{BCS}}(T), \tag{7}$$

where $B_0 = 100\,\mathrm{mT}$ and

$$R_{\mathrm{BCS}}(T) = \frac{A\omega^2}{T} \exp\left(-\frac{\Delta(T)}{k_B T}\right),$$

with the temperature dependence of Δ approximated as Ref. [9]

$$\Delta(T) = \Delta_0 \sqrt{\cos\left(\frac{\pi}{2}\left[\frac{T}{T_c}\right]^2\right)}.$$

This model can be fit to a dataset of Q-curves taken while cooling the bath using the following procedure:

- Fit A, Δ_0, and R_0 to the lowest field ($B_p = 10\,\mathrm{mT}$) points in the dataset, supposing no field-dependence ($\gamma_0 = \gamma = 0$) and no TFB
- Keep A, Δ_0, and R_0 fixed and fit γ_0 to the lowest temperature Q-curve, still assuming $\gamma = 0$

ISBN: 978-3-95450-234-9 ISSN: 2673-5504 doi:10.18429/JACoW-SRF2023-MOPMB050

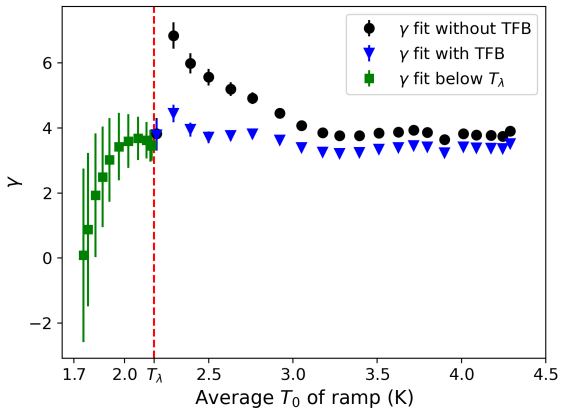

Figure 9: Fit parameter γ for all Q-curves in a cooldown of the 389 MHz mode of the 120 °C baked HWR.

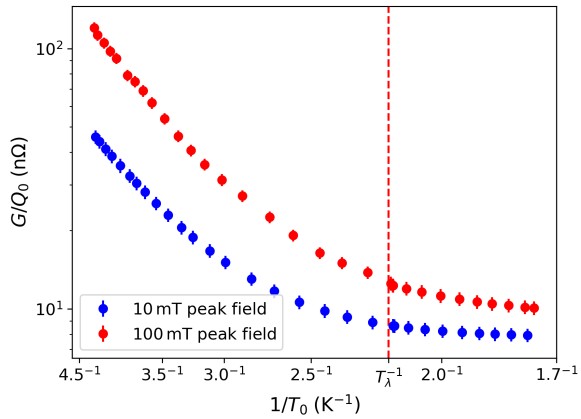

Figure 10: Average surface resistance G/Q_0 vs. inverse bath temperature $1/T_0$ for the 389 MHz mode of the 120 °C baked HWR after correcting for TFB.

- Fix A, Δ_0, R_0 and γ_0 and fit a different γ to each Q-curve of the cooldown

By attributing all Q-slope for the lowest temperature Q-curve to the temperature-independent part of R_s, the parameter γ is made to quantify the amount of Q-slope coming from the temperature-dependent part for every other Q-curve in the dataset. The fitting of γ can be done with or without accounting for TFB. In the latter case, the RF surface temperature is assumed $T = T_0$ everywhere. When $T_0 < T_\lambda$, it is assumed that there is no TFB.

An example of this procedure applied to coaxial cavity data is shown in Fig. 9. The gap between the γ's fit with and without TFB indicate the impact of TFB on each Q-curve. If all Q-slope in the dataset came from TFB, then the γ's fit with TFB would be close to zero. Our data shows that a significant portion of Q-slope comes from an intrinsic field-dependence of the temperature-dependent part of R_s.

When fit without TFB, γ shows a strong discontinuity at T_λ, but when TFB is taken into account, this discontinuity mostly disappears. The change in Q-slope at T_λ comes then from TFB, and not from the intrinsic properties of the superconductor.

Another way of seeing the effect of TFB on surface resistance measurements is to fit γ to each Q-curve with TFB, and use this γ to predict Q_0 for every B_p in that curve without TFB. In this way one obtains a TFB-corrected dataset like the one in Fig. 10, which does not show a jump in G/Q_0 at T_λ.

CONCLUSIONS

Boiling curves for niobium in saturated normal fluid liquid helium were measured for the first time and the effects of bath temperature and surface orientation are reported. Finite-element methods have been successfully implemented for fitting surface resistance models to cavity datasets to untangle the effects of TFB from field-dependence in R_s. A key finding of the preliminary work is that TFB contributes to Q-slope but does not fully explain the phenomenon. It is interesting to note that the effect of TFB on measured Q-slope becomes stronger at low temperatures due to reduced efficiency of boiling heat transfer. These tools will be used in future studies to assess the agreement of field-dependent models of surface resistance without the confounding effect of TFB.

ACKNOWLEDGEMENTS

We would like to thank the technical team at TRIUMF for their assistance in the boiling curve measurements, as well as National Research Council Canada for funding this work.

REFERENCES

[1] P. Kolb *et al.*, "Coaxial multimode cavities for fundamental superconducting rf research in an unprecedented parameter space," *Phys. Rev. Accel. Beams*, vol. 23, no. 12, p. 122 001, 2020. doi:10.1103/PhysRevAccelBeams.23.122001

[2] V. Palmieri, A. A. Rossi, S. Y. Stark, and R. Vaglio, "Evidence for thermal boundary resistance effects on superconducting radiofrequency cavity performances," *Supercond. Sci. Technol.*, vol. 27, p. 085 004, 2014. doi:10.1088/0953-2048/27/8/085004

[3] P. Bauer *et al.*, "Evidence for non-linear BCS resistance in SRF cavities," *Physica C*, vol. 441, pp. 51–56, 2006. doi:10.1016/j.physc.2006.03.056

[4] K. Mittag, "Kapitza conductance and thermal conductivity of copper niobium and aluminium in the range from 1.3 to 2.1 k," *Cryog.*, vol. 13, no. 2, pp. 94–99, 1973. doi:10.1016/0011-2275(73)90132-X

[5] F. Koechlin and B. Bonin, "Parametrization of the niobium thermal conductivity in the superconducting state," *Supercond. Sci. Technol.*, vol. 9, no. 6, pp. 453–460, 1996. doi:10.1088/0953-2048/9/6/003

ISBN: 978-3-95450-234-9 ISSN: 2673-5504 doi:10.18429/JACoW-SRF2023-MOPMB050

[6] N. Kaneyasu, F. Yasunobu, U. Satoru, and O. Haruhiko, "Effect of surface configuration on nucleate boiling heat transfer," *Int. J. Heat Mass Transfer*, vol. 27, no. 9, pp. 1559–1571, 1984. doi:10.1016/0017-9310(84)90268-0

[7] J. Ding, D. L. Hall, and M. Liepe, "Simulations of RF Field-induced Thermal Feedback in Niobium and Nb3Sn Cavities," in *Proc. SRF'17*, Lanzhou, China, Jul. 2017, pp. 920–924. doi:10.18429/JACoW-SRF2017-THPB079

[8] A. C. Polycarpou, *Introduction to the finite element method in electromagnetics,* Springer, 2005.

[9] T. P. Sheahen, "Rules for the energy gap and critical field of superconductors," *Phys. Rev.*, vol. 149, no. 1, pp. 368–370, 1966. doi:10.1103/PhysRev.149.368